



Airway proteins involved in bacterial clearance susceptible to cathepsin G proteolysis

M.M. Farberman, K.T. Akers, J.P. Malone, P. Erdman-Gilmore, R.R. Townsend and T. Ferkol

ABSTRACT: Serine proteases released from neutrophils are central to the pathogenesis of cystic fibrosis lung disease and are considered to be obvious therapeutic targets. Neutrophil elastase digests key opsonins present in the lung and disrupts phagocytosis, allowing bacteria to persist despite established pulmonary inflammation. We have found that cathepsin G, an abundant serine protease found in human and murine neutrophils, has other roles in the development of suppurative lung diseases. Murine models of endobronchial inflammation indicate that cathepsin G inhibits airway defences and interferes with the host's ability to clear *Pseudomonas aeruginosa* from the lung with effects distinct from neutrophil elastase. We hypothesise that differences in bacterial killing are due to defects in innate defences created by proteolysis.

Protein profiles of bronchoalveolar lavage of infected wild-type and cathepsin G-deficient mice were compared using two-dimensional polyacrylamide gel electrophoresis and tandem mass spectrometry.

Four proteins in bronchoalveolar lavage were cleaved by cathepsin G. Serum amyloid P component leaked into the lung during acute infection and was digested by cathepsin G. Its cleavage products had greater binding to lipopolysaccharide and interfered with phagocytosis.

These results indicate that cleaved serum amyloid P component acts as an anti-opsonin and interferes with bacterial clearance from the lung.

KEYWORDS: Bacteria, cystic fibrosis, infection, protease, serum amyloid P

The phagocytic system affords protection against bacterial invasion, yet it also contributes to epithelial cell injury and damage. Neutrophils possess several highly related serine proteases, including neutrophil elastase (NE) and cathepsin G (CG) [1]. These proteases are critical for neutrophil responses against infection, participating in intralysosomal degradation of engulfed bacteria [2]. However, large amounts of proteases escape from neutrophils during phagocytosis and apoptosis. The release of catalytically active enzymes can have harmful effects on the respiratory epithelium, and protease burden in suppurative lung diseases, including cystic fibrosis, overwhelms the existing antiprotease defence [3]. NE has long been considered pre-eminent in cystic fibrosis since this omnivorous enzyme plays several roles in the pathogenesis of lung disease [4], but other neutrophil-derived serine proteases could have

effects on airway defences. Considerably less is known about the physiological role(s) of other proteases, such as CG, but these enzymes could be relevant to the pathogenesis of cystic fibrosis lung disease. One of the most abundant proteins found in human and murine neutrophils [5] is CG, which can activate airway epithelial cells and stimulates secretion from airway submucosal glands [6]. CG is important for neutrophils to respond to chemotactic signals [7], and when intracellular it has direct antimicrobial activity against microorganisms [8].

Identification of candidate molecules degraded by serine proteases has historically been limited by technology that permitted only simultaneous analysis of a few individual proteins. The advent of proteomics now provides investigators with tools to interrogate hundreds of proteins in a single experiment. We previously reported that CG interferes with the host's ability to clear

AFFILIATIONS

Dept of Paediatrics and Internal Medicine, Washington University School of Medicine, St Louis, MO, USA.

CORRESPONDENCE

T. Ferkol
Division of Paediatric Allergy and Pulmonary Medicine
Dept of Paediatrics
Washington University School of Medicine
660 South Euclid Avenue
Mailbox 8116
St Louis
MO 63110
USA
E-mail: ferkol_t@kids.wustl.edu

Received:

Feb 06 2009

Accepted after revision:

July 09 2009

First published online:

Aug 13 2009

This article has supplementary material available from www.erj.ersjournals.com

Pseudomonas aeruginosa (PA01) from the murine lung, which we postulated was due to degradation of innate or adaptive defences at the airway surface [1]. Using these well-characterised murine models of acute bacterial endobronchitis, we tested this hypothesis using newer proteomic approaches. The data we present herein begin to define the mechanisms by which specific neutrophil-derived serine proteases contribute to pathogenesis of suppurative airway disease and lead to bacterial persistence.

EXPERIMENTAL METHODS AND MATERIALS

Animals

Protease-deficient ($ne^{+/+}cg^{-/-}$ and $ne^{-/-}cg^{-/-}$) mice previously created by homologous recombination were used in these experiments [9, 10]. Protease-sufficient mice ($ne^{+/+}cg^{+/+}$) of the same genetic background were used as controls, *i.e.* wild-type (WT) 129/SvJ strains. The genotype of individual animals was established by PCR amplification (Perkins Elmer Cetus, Norwalk, CT, USA) of genomic DNA using established protocols. All mice were maintained in micro-isolator units and housed in the Animal Resource Center at Washington University School of Medicine (St Louis, MO, USA).

Murine model of endobronchial inflammation

An adaptation of the agarose bead method was used to create a neutrophilic endobronchitis in mice [11]. Based on previous data examining maximum bacterial burden and inflammation in this infection model, bronchoalveolar lavage (BAL) was performed 3 days after infection using established techniques [11]. BAL fluid (BALF) cell counts were performed using established techniques, and marker pro-inflammatory cytokines were measured using commercially available ELISA kits (R&D Systems, Minneapolis, MN, USA) as per manufacturer's instructions.

Proteomics analysis of BALF using two-dimensional difference gel electrophoresis and nano-liquid chromatography-mass spectrometry

Samples were labelled with charge-matched cyanine dyes as previously described [12–14]. Each sample (50 μ g) was prepared in sample buffer (30 mM Tris-HCl pH 8.5, 7 M urea, 2 M thiourea, 4% 3-((3-Cholamidopropyl)dimethylammonio)-1-propanesulfonate) and labelled with 400 pmol Cy2, Cy3 or Cy5. All samples were equilibrated into immobilised pH gradient strips under 100 V followed by isoelectric focusing using a maximum of 10,000 focusing volts (Protean IEF cell; BioRad, Hercules, CA, USA). After focusing, proteins were reduced with dithiothreitol and alkylated with iodoacetamide. The IPG strip was then layered onto 10% polyacrylamide gels followed by sodium dodecyl sulphate polyacrylamide gel electrophoresis (SDS-PAGE) separation. Samples were imaged with a Typhoon Imager (GE Healthcare, Piscataway, NJ, USA) at the following specific excitation/emission wavelengths: 488/520 nm for Cy2, 520/580 nm for Cy3 and 620/670 nm for Cy5. The DeCyder (v. 6.5) software tools (GE Healthcare) were used for image analysis. The differential in-gel analysis (DIA) module was used to align and normalise images within each gel. The DIA module calculated abundance ratios using the normalisation algorithm [15]. Spots with slopes >1.1, areas <100 pixels, volumes <10,000 pixels and peak heights <100 pixels were excluded. For comparative pair-wise analyses of

features across different physical gels, the DIA data sets were analysed using the biological variation analysis module. Spot volumes were converted to ratios of a pooled internal standard. Spots were excised robotically (ProPic; Genomic Solutions, Huntingdon, UK) using a triangulation algorithm implemented with in-house software, and gel pieces were digested *in situ* with trypsin [16]. Samples were processed and analysed using matrix-assisted laser desorption/ionisation time-of-flight (MALDI-TOF)/TOF mass spectrometry (MS) (ABI-4700; Applied Biosystems, Foster City, CA, USA) [14]. The tandem MS spectra were used to search the National Center for Biotechnology Information protein database (downloaded on February 18, 2007) with the following constraints: MS tolerance, 50 ppm; and MS/MS tolerance, 0.200 ppm, with fixed modifications of cysteine residues (carbamidomethylation) and variable oxidation of methionine residues.

Immunoblot analyses of serum amyloid P in BALF

BALF samples (500 μ L) from infected mice were concentrated 16-fold using a 3,000 MWCO Microcon centrifugal filter device (Millipore Corporation, Bedford, MA, USA). Proteins were separated using SDS-PAGE and transferred onto poly(vinylidene fluoride) membranes using established approaches. The blots were blocked with TBS, pH 7.4, 0.03% TWEEN 20 and 10% (w/v) dry skimmed milk overnight at 4°C, then incubated at 21°C with rabbit anti-serum amyloid P (SAP) antibody (1:20,000; Abcam, Cambridge, MA, USA) followed by horseradish peroxidase (HRP)-conjugated, goat anti-rabbit immunoglobulin (Ig)G antibody (1:50,000; Sigma, St Louis, MO, USA). The membranes were washed, then SuperSignal Extended Duration Substrate (Pierce Biotechnology, Rockford, IL, USA) was applied for 5 min. Luminescence was detected by exposure to photographic film.

CG digestion of SAP

Human SAP (125 ng, 250 ng, 500 ng, 1,000 ng and 2,000 ng) (Sigma) was treated with increasing concentrations (0.2 μ M, 1 μ M, 5 μ M and 25 μ M) of excess CG (Elastin Products, Owensville, MO, USA) for 24 h at 37°C. Immunoblot analysis was performed on CG-treated and untreated SAP as previously described, except the secondary antibody was used at 1:1,000. Amersham ECL western blotting reagents (GE Healthcare, Piscataway, NJ, USA) were applied for 1 min to washed membranes. Luminescence was detected by exposure to photographic film.

SAP binding to *P. aeruginosa* lipopolysaccharide

Lipopolysaccharide (LPS) from *P. aeruginosa* 10 (1 μ g·mL⁻¹, Sigma) was applied to 96-well flat-bottomed ELISA plates and incubated at 37°C for 1 h, followed by a 16-h incubation at 4°C. The plates were washed with water containing 0.05% TWEEN 20, and blocked overnight with 200 μ L of PBS, 4% bovine serum albumin and 0.05% TWEEN 20 at 4°C. The plates were washed, and human serum samples incubated with increasing CG concentrations (10 μ M, 100 μ M and 1,000 μ M) overnight at 37°C were applied to each well for 16 h at 4°C. After additional washings, bound SAP was identified by sequential incubation with 1:5,000 rabbit anti-human SAP antibody (Lifespan, Seattle, WA, USA) and 1:10,000 HRP-conjugated, goat anti-rabbit IgG antibody (Sigma). Following washings, the plates were developed using the TMB microwell peroxidase substrate

system (KPL, Inc., Gaithersburg, MD, USA). The colorimetric reaction was stopped by addition of 100 μL of 1 M H_3PO_4 per well, and absorbance was measured using the VERSAmax microplate reader at 450 nm (Molecular Devices, Sunnydale, CA, USA).

Opsonophagocytosis of LPS incubated with cleaved SAP

HL-60 cells (promyelocytic leukaemia cells, CCL240; American Type Culture Collection, Rockville, MD, USA) were grown and differentiated as previously described [17]. SAP (10 μg) was cleaved with 100 nM CG as described previously. Cleaved SAP, untreated SAP and buffer control were incubated with PA01 for 15 min at 37°C. Differentiated HL-60 cells were mixed with the bacterial pellet and incubated for 90 min at 37°C. Gentamicin (1:100) was added for 1 h at 37°C. Following centrifugation, cells were washed three times with 200 μL of PBS and then centrifuged at $300 \times g$ for 8 min. HL-60 cells were then lysed with 10 μL of 0.1% Triton X-100, streaked on TSA plates, and examined for *P. aeruginosa* colonies after overnight incubation at 37°C.

Statistical analysis

Data are expressed as mean \pm SEM. Statistical comparisons between control and CG-deficient mice were made using the two-tailed unpaired t-test. For ELISA studies, statistical comparison of the effects of SAP, its digestion products and controls, single factor ANOVAs were used.

RESULTS

Animal model

To determine the mechanism by which CG interferes with bacterial clearance from the lung, syngeneic CG-deficient ($ne^{+/+}cg^{-/-}$) and CG-replete WT ($ne^{+/+}cg^{+/+}$) mice [10] were challenged with PA01-laden beads (fig. 1), which mimics the pathology seen in the cystic fibrosis lung. This endobronchitis model allows control and manipulation of the host's genetic background, as well as genotype and virulence factors

expressed by infecting organisms, variables that are difficult to evaluate in humans.

Lavage analyses

Before and after infection, cell counts and the histopathological appearance of the lungs were similar between mouse genotypes. There was no difference in neutrophil concentrations in BALF of uninfected WT and $ne^{+/+}cg^{-/-}$ mice (fig. 2), which indicates that neutrophil transmigration was unaffected by the absence of serine proteases. More importantly, the inflammatory cell composition of the BALF was virtually identical, which suggests that their contribution to proteins in the fluid was also similar. There was no difference in total protein or selected inflammatory mediator concentrations in BALF (total protein: WT $61.3 \pm 19.7 \mu\text{g}\cdot\text{mL}^{-1}$, $ne^{+/+}cg^{-/-}$ $65.2 \pm 5.1 \mu\text{g}\cdot\text{mL}^{-1}$; macrophage inflammatory protein-2: WT $96.1 \pm 14.2 \text{ ng}\cdot\text{mL}^{-1}$, $ne^{+/+}cg^{-/-}$ $69.1 \pm 19.7 \text{ ng}\cdot\text{mL}^{-1}$; keratinocyte chemoattractant: WT $6.0 \pm 0.8 \text{ ng}\cdot\text{mL}^{-1}$, $ne^{+/+}cg^{-/-}$ $7.0 \pm 0.5 \text{ ng}\cdot\text{mL}^{-1}$; and tumour necrosis factor- α , WT $2.1 \pm 0.23 \text{ ng}\cdot\text{mL}^{-1}$, $ne^{+/+}cg^{-/-}$ $1.5 \pm 0.17 \text{ ng}\cdot\text{mL}^{-1}$).

CG degradation of proteins in BALF

To determine the mechanism by which CG affects bacterial clearance from the airways, we examined profiles of proteins secreted into the infected lung using proteomic techniques. BALF from six identically treated syngeneic $ne^{+/+}cg^{-/-}$ mice and WT controls was collected after PA01 infection. Two-dimensional (2D)-PAGE analysis of BALF revealed a total of 1,571 gel features with 170 spots that were changed in volume by 2 SD or 2.6-fold difference between the two pooled samples. The number of features that showed increased or decreased spot volumes was approximately the same (82 versus 88). Many of the changes (indicated by the red gel features) were part of charge trains, which are characteristic of plasma proteins (fig. 3). Thus, we focused on individual, well-delineated gel features that changed by more than three-fold for our protein identification studies using MS, as illustrated by the identified gel feature (fig. 3). Features of interest were flagged in DIA

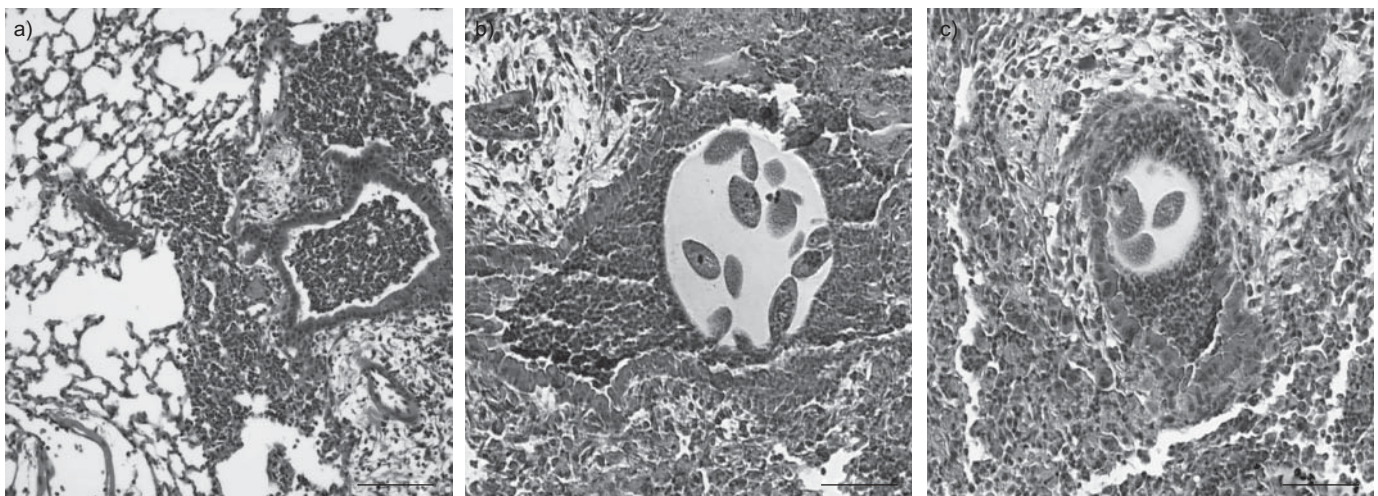


FIGURE 1. Photomicrographs of murine lungs 3 days after instillation of *Pseudomonas*-laden agarose beads. a) The histopathological features of the lungs that closely mimic the pathology present in the cystic fibrosis lung, including endo- and peribronchial inflammation and local extension into the airspace. Otherwise, the alveoli are relatively spared. Scale bar=200 μm . Photomicrographs showing bronchial sections from b) isogenic wild-type and c) cathepsin G-deficient ($ne^{+/+}cg^{-/-}$) mice following infection. Largely, there was no difference in the degree or extent of airway inflammation. Scale bars=100 μm .

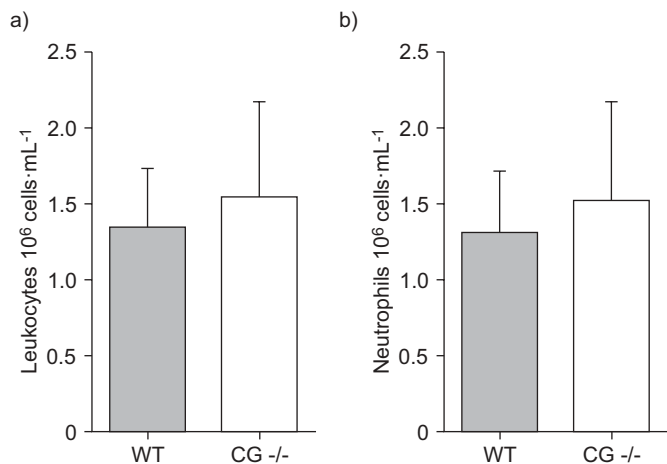
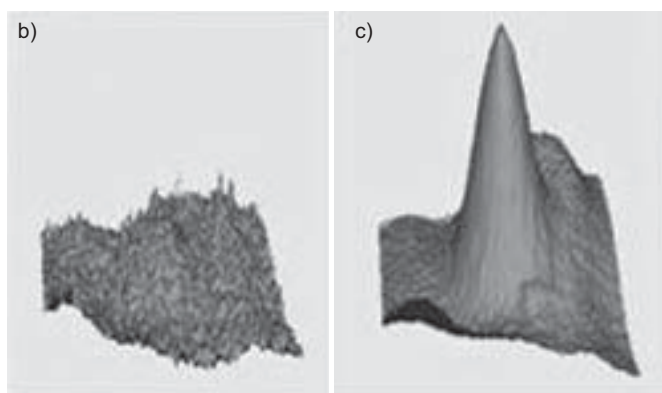
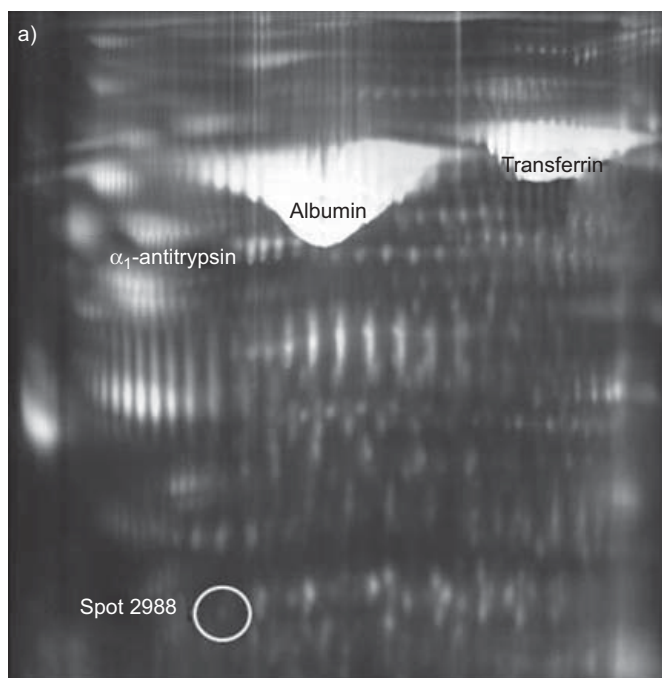


FIGURE 2. a) Leukocyte and b) neutrophil concentrations in the lungs from isogenic wild-type (WT) and cathepsin G (CG)-deficient ($ne^{+/+}cg^{-/-}$) mice after inoculation with *Pseudomonas*-laden beads. In both murine genotypes, there was a marked increase in lavage leukocyte concentration and absolute neutrophil counts after infection, but no difference in inflammatory phenotypes between CG-replete and CG-deficient cohorts (two-tailed unpaired t-test).



software, excised robotically and digested *in situ*. The peptides were analysed by tandem mass spectrometry using MALDI-TOF/TOF MS and database searching with MASCOT software. Proteins were identified in 23 gel features (see fig. 1 in the supplementary material), and four proteins were reduced (table 1). The most promising candidate degraded by CG in the lung, potentially involved in bacterial clearance, was SAP.

Presence of SAP in murine lung

SAP is expressed in murine hepatocytes as an acute-phase protein [18], and is secreted into circulation and extravascular tissues [19, 20]. We were able to detect SAP in both uninfected and infected murine serum (data not shown). Previous reports, however, failed to demonstrate SAP expression in the lung [21], and, using immunoblot analysis, we found SAP only in the BALF of infected mice ($ne^{-/-}cg^{-/-}$) and not in uninfected controls (fig. 4). These data suggest that SAP leaked from the serum into the airspace upon infection.

CG cleavage of SAP

Our proteomics data indicated that SAP was present in BALF of PA01-infected mice and susceptible to CG cleavage. We confirmed this finding by immunoblot analysis of SAP

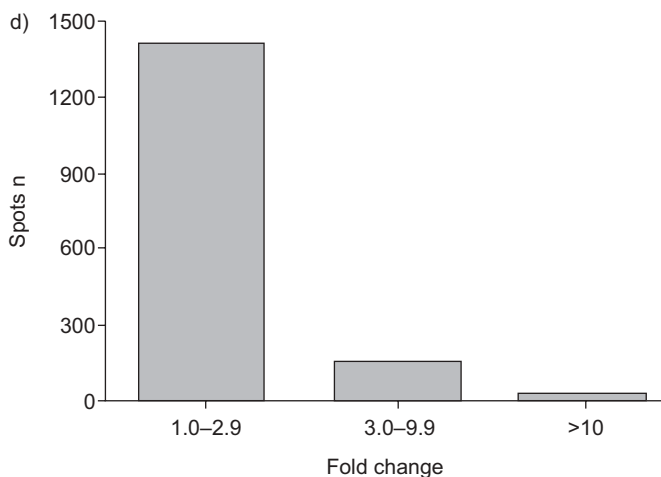


FIGURE 3. Two-dimensional (2D)-differential gel electrophoresis of bronchoalveolar lavage fluid from cathepsin G (CG)-deficient ($ne^{+/+}cg^{-/-}$) and isogenic wild-type (WT) littermate controls after *Pseudomonas* infection. a) Fluorophore-labelled proteins in bronchoalveolar lavage samples from WT and CG-deficient mice after infection, separated using 2D-differential gel electrophoresis. A region of interest was highlighted, which permitted precise excision and analysis of the candidate. The serum amyloid P location was identified (spot 2988). b, c) Fluorophore-labelled serum amyloid P peaks from b) WT and c) CG-deficient mice lavage fluid were quantitated and compared. d) Histogram showing distribution of relative spot intensities, expressed as fold change, comparing lavage fluid collected from infected WT and CG-deficient mice.

TABLE 1 Proteomic analysis of bronchoalveolar lavage fluid from isogenic wild-type (WT) and cathepsin G (CG)-deficient ($ne^{+/+}cg^{-/-}$) mice 3 days after infection, showing identified proteins susceptible to CG cleavage

Fold change	WT:CG ^{-/-}	Candidate function
Inter-α inhibitor proteins	3.59	Serine protease inhibitor; role in inflammation and wound healing
Selenium-binding protein	4.03	Regulation of cell proliferation and differentiation in lung
β_2-glycoprotein 1 precursor	3.61	Zymogen of serine protease involved in complement activation
Serum amyloid P component	3.21	Member of pentraxin family, opsonin and anti-opsonin
Sec 14-like protein	-8.56	Role in Golgi transport
Annexin A5	-3.50	Modulates cell signalling via Jak-Stat 1

following overnight incubation with increasing molar-excess CG. With increasing protease concentrations, digestion fragments were produced (fig. 5a). Similar fragments were seen when the concentration of CG was constant and the SAP concentration was increased (fig. 5b). These results conclusively demonstrate that SAP is proteolytically cleaved by CG.

CG cleavage alters the function of SAP

SAP binds to various forms of LPS, thus neutralising its biological effects and targeting it for removal [20]. We determined whether CG digestion altered SAP function and binding avidity to LPS. We examined untreated and CG-digested SAP binding to LPS using ELISA, and found that SAP fragments had greater binding to LPS than to the undigested protein (fig. 6). Moreover, we established that digested SAP fragments interfered with LPS-mediated phagocytosis by macrophages. SAP treatment reduced *P. aeruginosa* uptake by the HL-60 macrophage line *in vitro*, but phagocytosis was markedly inhibited when bacteria were pre-incubated with CG-digested SAP (fig. 7). These data indicate that SAP cleavage products act as anti-opsonins, and provide a potential mechanism by which CG inhibits *P. aeruginosa* clearance from the lung.

DISCUSSION

We have previously shown that CG interferes with the host's ability to eliminate *P. aeruginosa* from the murine lung [1]. In this study, we applied proteomic approaches to identify antimicrobial factor(s) in the lung susceptible to CG proteolysis and central to bacterial clearance in the airway. We found that SAP was important for pulmonary clearance of *Pseudomonas* in

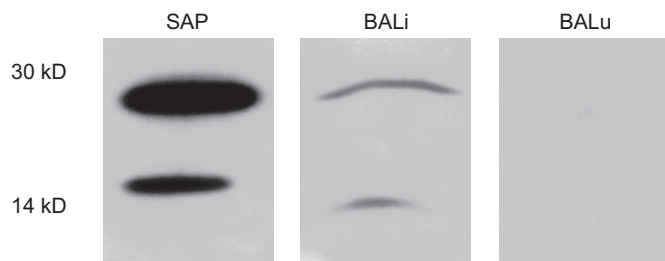


FIGURE 4. Presence of serum amyloid P (SAP) in murine bronchoalveolar lavage fluid. Bronchoalveolar lavage fluid collected from infected (BALi) or uninfected (BALu) CG-deficient mice ($ne^{+/+}cg^{-/-}$) were analysed using immunoblotting. The 30-kD SAP band was detected in BALi but not in BALu. Human SAP was used as a control.

syngeneic mouse models, and its cleavage products bind to *Pseudomonas* LPS, thus defining its role in bacterial opsonophagocytosis.

BAL provides a “window to the lungs” [22], allowing analysis of accessible cells and epithelial lining fluid (ELF), the thin fluid layer that covers the immediate airway surface which contains many proteins and mediators secreted by resident epithelial cells or diffused into the airway and alveoli. In disease, BALF is even more complex, since recruited immune cells, *e.g.* neutrophils, also contribute to the protein composition of ELF. Differences in genetic backgrounds or environmental influences

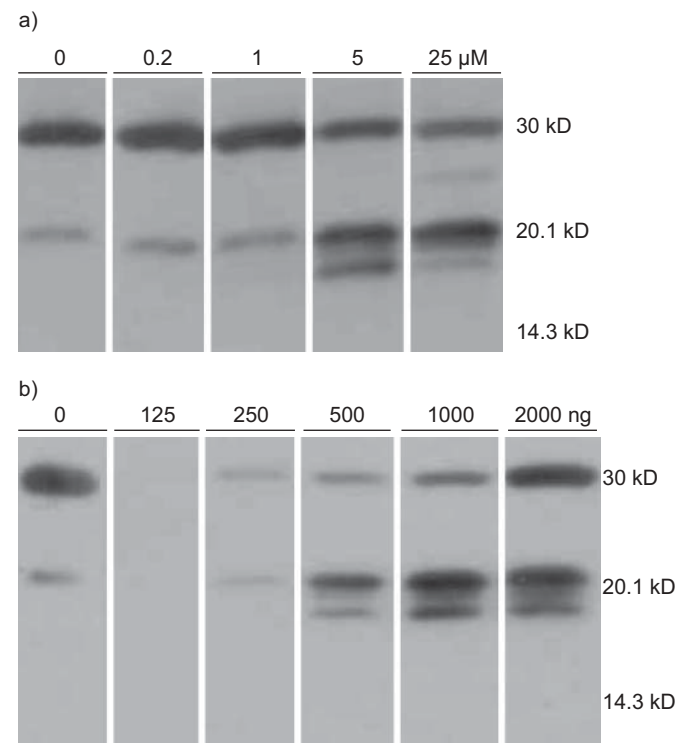


FIGURE 5. Immunoblot analysis of serum amyloid P (SAP) component cleavage by cathepsin G (CG). a) SAP (1,000 ng) isolated from human serum was treated with increasing concentrations of CG (0, 0.2, 1, 5 and 25 μ M). b) SAP (0, 125, 250, 500, 1,000 and 2,000 ng) isolated from human serum was treated with 5 μ M CG for 24 h at 37°C and analysed using sodium dodecyl sulphate polyacrylamide gel electrophoresis. Molecular weight standard is shown. The antibody detected a 25-kD band, consistent with the predicted size of SAP, but also several smaller, discrete, cleaved fragments following digestion.

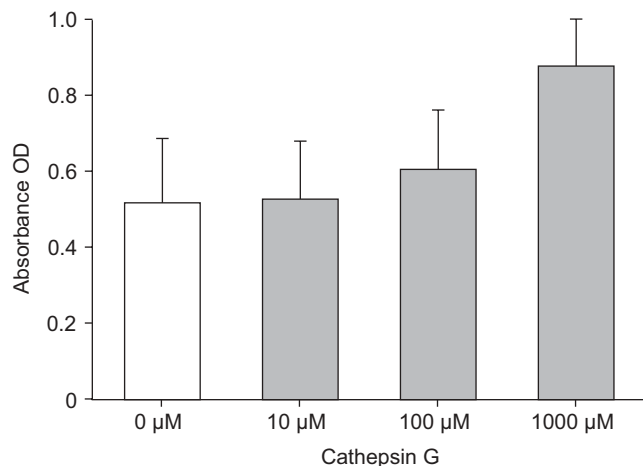


FIGURE 6. ELISA demonstrating that cathepsin G cleavage of serum amyloid P enhanced its binding to *Pseudomonas aeruginosa* lipopolysaccharide. OD: optical density. n=6. One-way ANOVA, $p=0.002$.

on subjects can account for differences in protein expression and confound analyses. The murine models used in these studies have the advantage that such factors can be controlled or manipulated.

Typically, proteomic analysis of lung disease has been performed on conditioned culture media or cellular lysates [23]. The earliest proteomic profiling of BALF was published 30 yrs ago, and identified proteins in patients with alveolar proteinosis. Since that time, analyses have been performed on respiratory samples collected from patients with various lung diseases, including cystic fibrosis [24]. ELF dilution has been a problem, but with technological advances, more proteins are now detectable. Many proteins found in the lavage are plasma proteins that diffused into the airspace, including IgG, α_1 -antitrypsin, albumin and, as we describe, SAP. Using newer protocols, we were able to identify candidate proteins that are susceptible to CG degradation. 2D-difference gel electrophoresis (DIGE) is a multiplexed proteomics method, which enables the simultaneous comparison of as many as three experimental conditions in the same physical gel. This approach avoids the well-recognised inter-gel variability and eliminates the imperfect warping process to align gel spots across gels [25]. The resulting differential protein expression data can be interpreted with greater confidence with fewer gels.

In these experiments, we collected BALF from PA01-infected CG-deficient and replete mice. The CG^{-/-} mice used in these experiments have no detectable CG protein or enzymatic activity in their neutrophils. BALF from both murine cohorts had similar profiles of recruited inflammatory cells, indicating that ne^{+/+}cg^{-/-} neutrophils can migrate into the lung in response to *Pseudomonas* infection. Differences in neutrophil concentrations or secreted proteins released into the respiratory ELF, along with those secreted from airway epithelia and alveoli, could have influenced our results. However, the concentration of inflammatory cells and secreted marker proteins were similar in the BALF from ne^{+/+}cg^{-/-} and WT mice after infection.

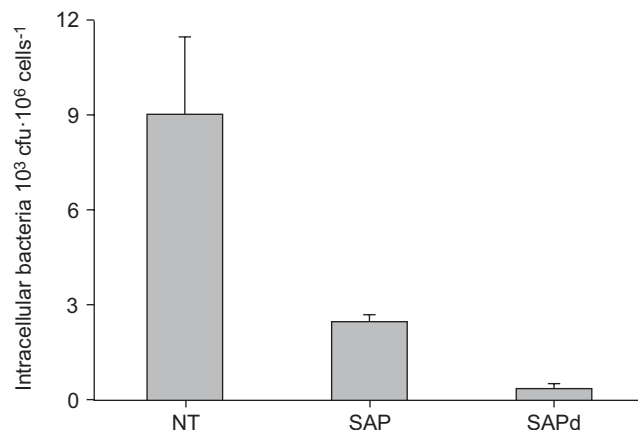


FIGURE 7. Opsonophagocytosis assay comparing *Pseudomonas aeruginosa* uptake by HL-60 cells after no treatment (NT), incubation with serum amyloid P (SAP) or SAP digested with cathepsin G (SAPd), showing that proteolytic cleavage of SAP further inhibits the phagocytosis of *P. aeruginosa* by macrophages *in vitro*. n=4–6. One-way ANOVA, $p=0.002$.

2D-DIGE analysis of murine BALF revealed a limited number of proteins that were digested or upregulated by CG. The most promising candidate identified was SAP, a member of the pentraxin family of proteins. It is a highly conserved glycoprotein consisting of 10 identical, noncovalently linked 25-kD subunits arranged in two pentameric rings [19]. In mice, SAP is the main acute-phase protein [19]. In humans, it is constitutively expressed with circulating levels ranging from 30 to 50 $\mu\text{g}\cdot\text{mL}^{-1}$ that increase during sepsis [19]. The physiological function of SAP is still unclear, though it appeared to exert its effect by binding to host- or pathogen-derived cellular debris [19]. Evidence obtained from SAP-deficient mice indicated that SAP may be protective in the presence of bacteria to which it does not bind, such as smooth strains of *Escherichia coli*, as shown by increased mortality of these mice after infection [26]. Conversely, SAP can act as an anti-opsonin during infections with bacteria that it binds, such as rough *E. coli*, by reducing its ability to be phagocytosed and killed [26].

BALF from patients with cystic fibrosis reveals an intense endobronchial inflammatory process, characterised by high neutrophil concentrations, even in patients with mild disease [27]. Once in the airway, neutrophils release high concentrations of serine proteases and extracellular, catalytically active enzymes, which have harmful effects on the respiratory epithelium. Overlapping with other proteases, CG has numerous substrates in the cystic fibrosis lung and has been shown to cleave components of the extracellular matrix, including collagen, fibronectin and elastin [28]. Moreover, it regulates innate immunity and inflammation through chemokine amplification, cleavage of cell-surface bound cytokine receptors, and proteolytic inactivation of collectins, cytokines and chemoattractants [29].

Because of its clear association with the pulmonary deterioration of cystic fibrosis patients and its ability to incite an intense neutrophilic response in the airway, *P. aeruginosa* was chosen for these investigations [11]. It is important to note that the inoculation of the lungs with PA01 embedded within agar

beads is not a model of initial infection, but simply a means to elicit neutrophilic influx into the mouse lung. Consequently, we were unable to address questions regarding the initial colonisation and retention of bacteria in the lung early in the development of cystic fibrosis lung disease. This model, however, does permit examination of the inflammatory response and the effect of CG on novel candidate molecules in the infected lung. Nevertheless, we cannot exclude the possibility that other proteases impact bacterial clearance from the lung. Although neutrophil proteases have different substrate specificities *in vitro*, their physiological effects *in vivo* may be redundant.

A circulating protein, SAP can be found in other body compartments. Other investigators were unable to demonstrate SAP expression in LPS-treated lungs [21], and it was undetectable in BALF from uninfected *ne^{-/-}cg^{-/-}* mice. SAP was found only in the BALF of *P. aeruginosa*-infected mice, suggesting that SAP leaks from the serum and enters the airspace after acute infection. Investigators have previously shown that amyloid P, an aggregated tissue form of SAP, is cleaved by neutrophil-derived enzymes [30]. We advanced this observation by demonstrating that CG cleaves SAP into several smaller fragments, thereby enhancing its ability to bind to *Pseudomonas* LPS and prevent phagocytosis by macrophages. These data indicate that SAP acts as an anti-opsonin in this setting. It is also possible that CG may digest other proteins involved in lung defences that are difficult to detect in 2D-gel separations.

In conclusion, few proteins are specifically digested by CG in BALF of infected mice, including SAP. CG cleavage of SAP renders it anti-opsonic, as evidenced by increased binding of SAP to *Pseudomonas* LPS and inhibition of phagocytosis *in vitro*, thus sequestering it within the lung and potentially contributing to persistent infection in cystic fibrosis.

SUPPORT STATEMENT

This research was supported by the Cystic Fibrosis Foundation, National Institutes of Health (R01 HL08265), National Centers for Research Resources of the National Institutes of Health (P41RR00954), and the Ruth L. Kirschstein National Research Service Award (2 T32 HL007873) from the National Heart, Lung, and Blood Institute (all Bethesda, MD, USA).

STATEMENT OF INTEREST

None declared.

REFERENCES

- Sedor J, Hogue L, Akers K, *et al.* Altered clearance of *Pseudomonas aeruginosa* from lungs of mice deficient in cathepsin-G. *Pediatr Res* 2007; 61: 26–31.
- Thorne KJ, Oliver CR, Barrett AJ. Lysis and killing of bacteria by lysosomal proteinases. *Infect Immunol* 1976; 14: 555–563.
- O'Connor CM, Gaffney K, Keane J, *et al.* Alpha 1-proteinase inhibitor, elastase activity, and lung disease severity in cystic fibrosis. *Am Rev Respir Dis* 1993; 148: 1665–1670.
- Birrer P, McElvaney NG, Rudeberg A, *et al.* Protease-antiprotease imbalance in the lungs of children with cystic fibrosis. *Am J Respir Crit Care Med* 1994; 150: 207–213.
- Travis J. Structure, function, and control of neutrophil proteinases. *Am J Med* 1988; 84: 37–42.
- Schuster A, Fahy JV, Ueki I, *et al.* Cystic fibrosis sputum induces a secretory response from airway gland serous cells that can be prevented by neutrophil protease inhibitors. *Eur Respir J* 1995; 8: 10–14.
- Lomas DA, Stone SR, Llewellyn-Jones C, *et al.* The control of neutrophil chemotaxis by inhibitors of cathepsin G and chymotrypsin. *J Biol Chem* 1995; 270: 23437–23443.
- Shafer WM, Shepherd ME, Boltin B, *et al.* Synthetic peptides of human lysosomal cathepsin G with potent antipseudomonal activity. *Infect Immun* 1993; 61: 1900–1908.
- MacIvor DM, Shapiro SD, Pham CT, *et al.* Normal neutrophil function in cathepsin-G-deficient mice. *Blood* 1999; 94: 4282–4293.
- Lopez-Boado YS, Espinola M, Bahr S, *et al.* Neutrophil serine proteinases cleave bacterial flagellin, abrogating its host response-inducing activity. *J Immunol* 2004; 172: 509–515.
- van Heeckeren AM, Tscheikuna J, Walenga RW, *et al.* Effect of *Pseudomonas* infection on weight loss, lung mechanics, and cytokines in mice. *Am J Respir Crit Care Med* 2000; 161: 271–279.
- Unlu M, Morgan ME, Minden JS. Difference gel electrophoresis: a single gel method for detecting changes in protein extracts. *Electrophoresis* 1997; 18: 2071–2077.
- Tonge R, Shaw J, Middleton B, *et al.* Validation and development of fluorescence two-dimensional differential gel electrophoresis proteomics technology. *Proteomics* 2001; 1: 377–396.
- Bredemeyer AJ, Lewis RM, Malone JP, *et al.* A proteomic approach for the discovery of protease substrates. *Proc Natl Acad Sci USA* 2004; 10: 11785–11790.
- Alban A, David SO, Bjorkesten L, *et al.* A novel experimental design for comparative two-dimensional gel analysis: two-dimensional difference gel electrophoresis incorporating a pooled internal standard. *Proteomics* 2003; 3: 36–44.
- Havlis J, Thomas H, Sebela M, *et al.* Fast-response proteomics by accelerated in-gel digestion of proteins. *Anal Chem* 2003; 75: 1300–1306.
- Romero-Steiner S, Libutti D, Pais LB, *et al.* Standardization of an opsonophagocytic assay for the measurement of functional antibody activity against *Streptococcus pneumoniae* using differentiated HL-60 cells. *Clin Diagn Lab Immunol* 1997; 4: 415–422.
- Cho K, Pham TN, Crivello SD, *et al.* Involvement of CD14 and toll-like receptor 4 in the acute phase response of serum amyloid A proteins and serum amyloid P component in the liver after burn injury. *Shock* 2004; 21: 144–150.
- de Haas CJC, van der Tol ME, Van Kessel KPM, *et al.* A synthetic lipopolysaccharide-binding peptide based on amino acids 27–39 of serum amyloid P component inhibits lipopolysaccharide-induced responses in human blood. *J Immunol* 1998; 161: 3607–3615.
- de Haas CJC, van der Zee R, Benaisa-Trouw B, *et al.* Lipopolysaccharide (LPS)-binding synthetic peptides derived from serum amyloid P component neutralize LPS. *Infect Immun* 1999; 67: 2790–2796.
- Vernooy JHJ, Reynaert N, Wolfs TGAM, *et al.* Rapid pulmonary expression of acute-phase reactants after local lipopolysaccharide exposure in mice is followed by an interleukin-6 mediated systemic acute-phase response. *Exp Lung Res* 2005; 31: 855–871.
- James DG, Rizzato G, Sharma OP. Bronchopulmonary lavage (BAL): a window of the lungs. *Sarcoidosis* 1992; 9: 3–14.
- Wattiez R, Falmagne P. Proteomics of bronchoalveolar lavage fluid. *J Chromatogr B Analyt Technol Biomed Life Sci* 2005; 815: 169–178.
- Ollero M, Brouillard F, Edelman A. Cystic fibrosis enters the proteomics scene: new answers to old questions. *Proteomics* 2006; 6: 4084–4099.
- Zhou G, Li H, DeCamp D, *et al.* 2D differential in-gel electrophoresis for the identification of esophageal scans cell cancer-specific protein markers. *Mol Cell Proteomics* 2002; 1: 117–124.
- Noursadeghi M, Bickerstaff MCM, Gallimore JR, *et al.* Role of serum amyloid P component in bacterial infection: protection of host or protection of the pathogen. *Proc Natl Acad Sci USA* 2000; 97: 14584–14589.

- 27** Konstan MW, Hilliard KA, Norvell TM, *et al.* Bronchoalveolar lavage findings in cystic fibrosis patients with stable, clinically mild lung disease suggest ongoing infection and inflammation. *Am J Respir Crit Care Med* 1994; 150: 448–454.
- 28** Reilly CF, Travis J. The degradation of human lung elastin by neutrophil proteinases. *Biochim Biophys Acta* 1980; 621: 147–157.
- 29** Bank U, Ansorge S. More than destructive: neutrophil-derived serine proteases in cytokine bioactivity control. *J Leukoc Biol* 2001; 69: 197–206.
- 30** Landsmann P, Rosen O, Pontet M, *et al.* Binding of human serum amyloid P component (hSAP) to human neutrophils. *Eur J Biochem* 1994; 223: 805–811.